EXACT SOLUTION FOR THE ENERGY DISTRIBUTION IN A FLAT ABSORBER OF A LINEAR PARABOLIC COLLECTOR

Manoel H. O. P. Filho[1,2], Naum Fraidenraich[1] and Olga C. Vilela[1]

[1] Federal University of Pernambuco, Nuclear Energy Dept., Recife (Brazil)

[2] Federal Institute of Education, Science and Technology of Pernambuco, Pesqueira (Brazil)

Abstract

This work presents a new approach to obtain the energy distribution in a flat absorber of a linear parabolic concentrator. The bright distribution of incident light (I(φ)) with angular aperture (φ_s) is determined by the beam rays with angle ($\varphi \leq \varphi_s$). The angle (θ) between the axis of the beam reflected in the parabolic surface and the parabola axis defines the relative position of the ray in the reflector. It is proposed a graphical representation for the (φ-θ) relation, associated with the positions (y) in the absorber (isolines). The diagrammatic representation allows visualizing which positions (y) in the absorber are total or partially illuminated by the parabolic reflector. Simulations of energy distribution in the absorber were implemented using different sun bright distributions. The illumination percentage along the absorber is also presented. Comparison with results of other models available in the literature shows a good agreement.

1. Introduction

The issue of light distribution in an absorber of a concentrator collector has been oftentimes treated in the scientific works in analytical form [4, 6, 7] or using ray tracing approach [2, 8]. The current progress in the concentrator technology used by both photovoltaic (multijunction cells) and thermal (SEGS) systems has revitalized its importance, especially in what refers to the optimization of concentrators design. This work, based in [5] shows a new approach to obtain the energy distribution in a flat absorber.

The bright distribution and geometrical equations are treated, at first, separately. The procedure allows using any bright distribution model and also experimental bright distributions. It also permits to perform analysis about the contributions of the segments of the parabola surface to the absorber illumination.

The proposed procedure incorporates all solar disc information to produce the radiation profile in the concentrator absorber region. A diagrammatic representation of the solution has been elaborated in order to facilitate both model comprehension and visualization of radiations profiles, considering deviations from the ideal condition.

The solar radiation that enters in the concentrator aperture is characterized by a conic beam of rays whose angular half aperture is equal to (φ_s) and its bright distribution is determined by the beam ray intensity (I), which depends on the angle (φ) within the angular aperture. The angle (φ_s) depends on the apparent sun width.

The ray energy intensity (I) in a determined point (y) of the absorber depends on the angles (θ) and (φ). The angle (θ) is defined between the cone central ray which is reflected by the parabola surface and the concentrator axis (Fig. 1). The angle (φ) is then associated to the beam that reflects with an angle (θ) and reaches the absorber in a determined point (y).

The model was developed to a linear focal parabolic concentrator and a flat absorber located in the focal region. Cylindrical concentrators deviate rays which are at the transversal surface to the concentrator axis. For this reason, only the projection of the rays in the transverse plane is analyzed. Under this condition, it is enough to consider a flat cone with half-angle aperture of (φ_s).
Geometries similar to the parabolic concentrator can be analyzed with the same model, with the single condition that the incident rays at the aperture perform only one reflection before reaching the absorber.

2. Development

The incident radiation in a parabolic cavity can be represented by a ray package ($+\varphi_s$, $-\varphi_s$) symmetrically distributed around a central ray. Analyzing the parabola´s plan, each ray from the package is identified by an angle (φ), formed by the ray and its beam axis. In the surface of the parabolic cavity it is defined the angle (θ), as the angle between the reflected beam axis and the axis of the parabola (Fig. 1), P1 and P2 are points where the ray reaches the parabola's surface. The flat absorber has an infinity length and width (W); and it is perpendicular to the parabola axis that contains its focus (F).

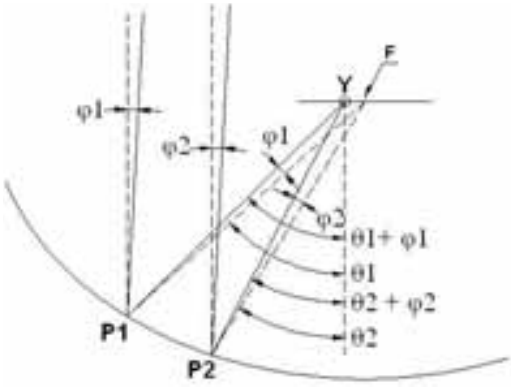

Fig. 1 – Parabola angles configuration in the focal plane.

In Fig. 1 it was arbitrated that (φ) is positive for rays situated on the left of the beam and negative for rays on the right of the beam. The angles (θ) are considered positive on the right of the parabola and negative on the left. The values of (y) are positive on the right of the focus and negative on the left.

The relationship between the point (y) where the ray reaches the focal plane and the angles (θ) and (φ) is given by (eq. 1).

$$y = \frac{r.\tan(\varphi).\sec(\theta)}{1-\tan(\varphi).\tan(\theta)}$$

(eq. 1)

r is the distance between the focal point and a point in the reflecting surface reached by a specific beam.
The eq. 1 leads to the same equation described by [3] that presents the total image length in the focal plane formed by a parabola with a rim angle (θ_r), a rim radius (r_r) and illuminated by a solar cone with a half solar angle (φ_s) (eq. 2).

$$W = \frac{2.r_r.sen(\varphi_s)}{\cos(\theta_r + \varphi_s)}$$

(eq. 2)

As mentioned before, the position (y) in the absorber will be reached by rays defined by an angle (φ) which belongs to a beam that was reflected by the parabola surface producing an angle (θ) with its axis. The angle (θ) defines the beam intersection point to the parabola. The angle (φ) defines a particular ray of this beam that reaches the point (y). A practical representation, shown in Fig. 2, allows visualizing the behavior of the rays that reach a point (y). The positions (y) are represented in the form of isolines.

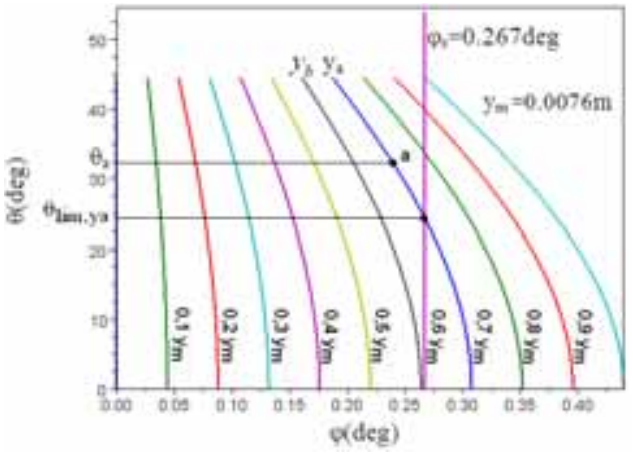

Fig. 2 – Set of values (θ – φ) that reaches the absorber in a point (y = constant) that it´s used as every curve parameter.

The angle (θ) is represented in the vertical axis of Fig. 2 and the angle (φ) is represented in the horizontal axis on the same figure. The values of (θ) vary since (0) up to the rim angle (θ_r), the values of (φ) vary from zero up to the sun half aperture (φ_s). The traced graphs are the geometrical place of the pair (θ – φ) that reaches the point (y) in the absorber (isolines). The parameter that corresponds to each isoline is exactly the place (y) reached by rays (θ – φ). For each value of the angle (θ) there is a unique value of (φ) that reaches the point (y) in the absorber.

The diagram of the Fig. 2 was plotted for a parabola with aperture of 1.64m and focal distance of 1m which results in y_m = 0.0076m (W = 0.0152 m). A set of 10 isolines referred to values of y, varying from 0 to y_m, is plotted in steps of 0.1 y_m. The graph shows one side of the parabola (θ > 0, right side) and points (y) in the right side of focus (F). These points are reached by rays with angle (φ > 0), defined as counterclockwise with respect to the beam axis (left side). The diagram for angles (θ < 0) is gotten using symmetry to the axis represented by the line (φ = 0).

The vertical line shown in the graph of Fig.2, indicates the maximum half angle of the beam (φ_s = 0.267 deg). This line defines two regions in the graph. In the left (abscissa, $\varphi \leq \varphi_s$) the (y) isolines that do not cross the line ($\varphi = \varphi_s$) represent portions of the absorber which receive incident beam contributions on the entire parabola.

The isolines that cross the line ($\varphi = \varphi_s$) represent a region that receives partial contribution of the parabola. In the Fig. 2 and for y = 0.6 y_m; the angle ($\theta_{lim,\ ya}$) separates the region of the parabola that contributes to illuminating the point (y_a) with ($\theta > \theta_{lim,\ ya}$) from the region that does not contribute ($\theta < \theta_{lim,\ ya}$). All points located on the left of the abscissa ($\varphi > \varphi_s$) receive partial illumination from the parabola.

Both partial and total illumination region in the absorber can be identified in the following way: the points in the absorber that receive total illumination from the parabola are in the interval ($0 \leq y \leq y_b$); the point y_b can be calculated using eq. 3.

$$y_b = f.\tan(\varphi_s)$$

(eq. 3)

(f) is the parabola focal length. This position in the absorber is defined by the isoline tangent to the vertical line (φ_s = 0.267 deg) in (θ =0), for the parabola used in the example (f = 1), $y_b = 0.606 y_m$.

The illuminated upper limit region of the absorber is defined by the value (y_m) equals to W/2 (absorber half length) and corresponds to the intersection of the vertical line (φ_s) with the isoline (y_m) (eq. 2). This absorber region is illuminated by the extreme rays that reach the concentrator rim. The absorber region between the

points (y_b) and (y_m) is partially illuminated by the incident rays in the parabola and arises, in all cases, and independently of the bright distribution of incident radiation, a descending illumination profile. This is also valid, for example, for a uniform bright profile.

The previous considerations can be visualized in (Fig. 3). The absorber region located between the focus and (y_b) receives contributions from entire parabolic surface. The absorber region ($y \geq y_b$) represented by the isolines that cross the vertical line (φ_s = 0.267 deg) receives rays that reaches only a part of the parabola. For instance, the interval ($y_a - y_m$), distant from the parabola focus (detached region) is illuminated only by the rays from the region ($p_a - p_r$) in the parabola surface.

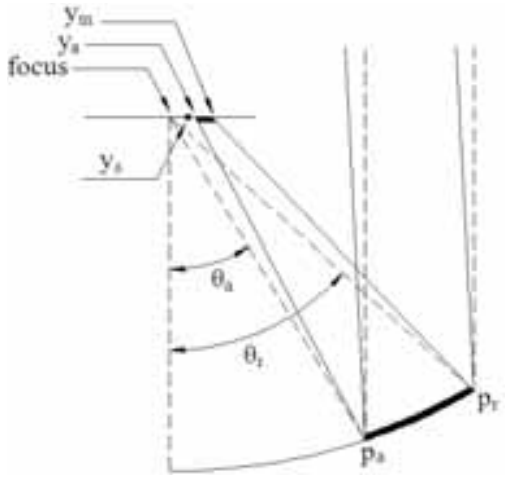

Fig. 3 – Details of focal region illumination.

The graphs in the Fig. 4 show, in an entire form, all the parabolic surface since $-\theta_r$ until θ_r, representing the total absorber extension since $-y_m$ (-W/2) until y_m (W/2), where y_m (W/2) is a half part of the maximum absorber length, calculated with the eq. 2.

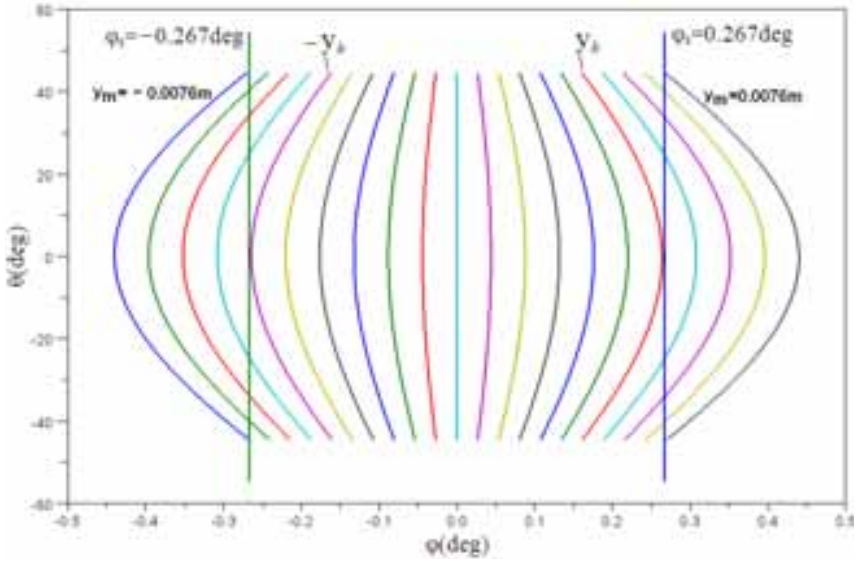

Fig. 4 – Parabola entire graph.

In a general form, the isolines in Fig. 4 that fit totally inside the two vertical lines, which indicate the solar cone limit ($-\varphi_s$ to φ_s), represent the absorber points reached by all rays from the solar beam. However, the isolines that cross these vertical lines represent absorber points (region between y_b and y_m (W/2) in Fig. 3) partially reached by the solar beam. The isolines out of the region delimited by the referred lines represent the points in the absorber not illuminated by the solar beam (region beyond y_m).

2.1 Determination of the energy distribution in the absorber

The incident energy in the point (y) is accounted as the contributions of all reflected rays in the band of the angle (θ) that have bright intensity I(φ). (φ) is the associated to (θ) for the parameter (y). This relation is shown in the eq. 4.

$$\tan(\varphi) = \frac{y}{|y.\tan(\theta)| + r.\sec(\theta)}$$

(eq. 4)

The radiation intensity I(y) reaching a determined point (y) will be, therefore, the addition of all parabola contribution, represented by eq. 5.

$$I(y) = \int_{-\theta_r}^{+\theta_r} I(\varphi(\theta, y)).\rho.\cos(\theta + \varphi(\theta, y)).d\theta$$

(eq. 5)

The I(φ(θ,y)) term is the radiation intensity variation inside the solar beam, in which (φ) representing the function φ = φ(θ,y). Any theoretical or experimental bright distribution can be used, for example, the proposed in [1] or [10].
The cos(θ+φ(θ,y)) term represents the cosine of the angle formed by the ray and the absorber normal (Fig. 1).
φ = φ(θ,y) is the function already described (eq. 4).
ρ represents the mirror reflectivity, and unitary value was used in the simulations.

To determine the local concentration in each point (y), it was used the flux concentration definition (C_{flux}) described by [9], as being the ratio between the flux in the absorber ($I_{absorber}$) (that is equal to I(y)) and the flux at the aperture ($I_{aperture}$) (eq. 6).

$$C_{flux}(y) = \frac{I(y)}{I_{aperture}}$$

(eq. 6)

$I_{aperture}$ was considered as being the sum of contributions of each ray defined by (φ) inside the solar beam (eq. 7), were I(φ) represents the solar beam radiation intensity or bright function.

$$I_{aperture} = \int_{-\varphi_s}^{+\varphi_s} I(\varphi).\cos(\varphi).d\varphi$$

(eq. 7)

3. Results

Using the described model, it was obtained the energy distribution in a flat absorber of a parabolic cavity with a focal length of 1m, aperture of 1.64 m and rim angle of 44.5 deg.

The Fig. 5 shows the concentration distribution, in which, the optical deviation was not considered and the reflectivity coefficient is equal to one.

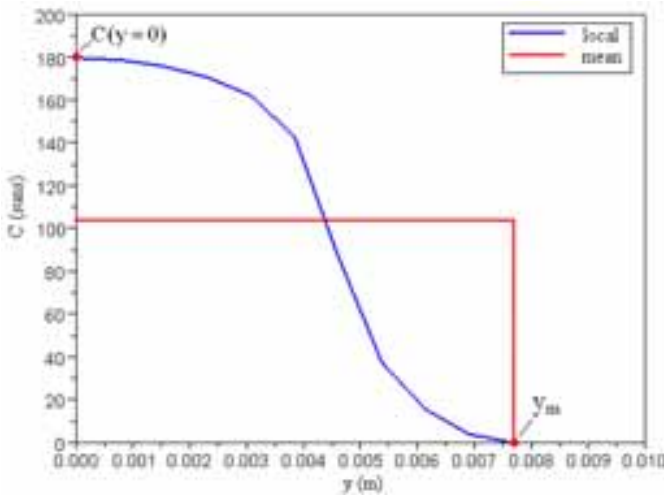

Fig. 5 – Energy distribution along by absorber.

The distribution shown in Fig. 5 (blue) was obtained using the bright distribution presented by [10]; the red graph represents the average concentration attained, 104.8 suns, that is a value equivalent to the calculated using eq. 8 [3].

$$C_{geom} = \frac{sen\theta_r \cos(\theta_r + 0{,}267)}{sen(0{,}267)} - 1$$

(eq. 8)

It can be verified that the maximum concentration reached is 179.8 suns (point C(y=0) in Fig. 5); the energy is distributed up to the maximum length (y_m), which is defined by the reflection of rays at the edge of the parabola. Its value is 0.0076m (y_m point, Fig. 5), providing a total image length of 0.015m, as calculated using the eq. 2.

The local concentration in the absorber center (C(y=0)) can be determined using the eq. 9.

$$C(y=0) = \frac{I(\varphi = 0).\rho.\sin(\theta_r)}{\int_0^{\varphi_s} I(\varphi).\cos(\varphi)\,d\varphi}$$

(eq. 9)

It depends on the bright distribution model (I(φ)) and its numerical integration.
For the constant bright distribution (eq. 10)

$$C(y=0) = 214.5\ .\rho.\ \sin(\theta_r)$$

(eq. 10)

For the bright distribution presented in [10] (eq. 11)

$$C(y=0)=257.3\ .\rho.\ \sin(\theta_r)$$

(eq. 11)

For the bright distribution presented in [1] (eq. 12)

$$C(y=0)=248.3\ .\rho.\ \sin(\theta_r)$$

(eq. 12)

Any bright can be used to get the maximum concentration in the absorber center.

The illumination of the absorber using four bright distributions is shown in the Fig. 6. The same parabola characteristics described before was used. The blue graph (Rabl) was performed using the bright distribution presented by [10]. The green (Constant) uses the constant bright distribution, the red (Gaussian) was obtained using a Gaussian bright distribution and the cyan (Abetti) uses the bright distribution presented by [1]. The entire absorber is shown.

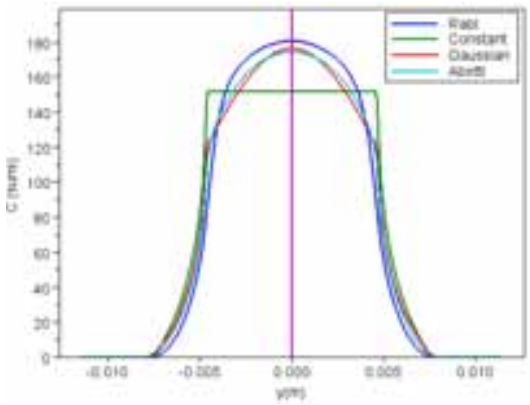

Fig. 6 – Energy distribution using four different bright distributions, showing the entire absorber.

It can be verified that Abetti and Gaussian are very similar. The distribution indicated as Rabl provides higher values of energy in the central region of the absorber and it will be considered as a referential to the following comparisons. For the maximum concentration (absorber centre), the constant distribution produced a value 15% less than the Rabl, the Gaussian got 2.3% less and Abetti got 3.4% less. For the mean quadratic error, the constant distribution presented 18.5 suns, the Gausian presented 9.4 suns and Abetti has 6.8 suns of deviation from Rabl distribution.

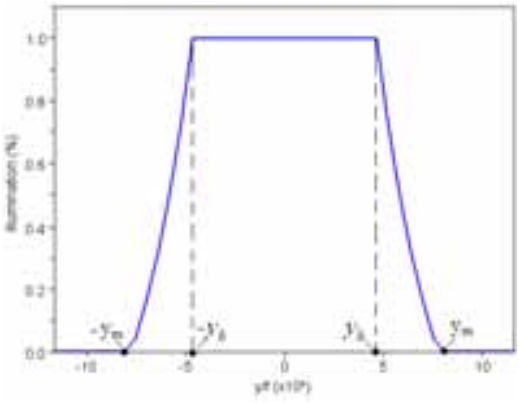

Fig. 7 – Illumination percentage of each point of the absorber.

The Fig. 7 shows illumination percentage of each point of absorber gotten using any bright distribution; it detaches the three important regions commented before, the region between the focus (y = 0) and (y_b) reached, as described, by all rays from the solar beam that reflects in all parabolic surface, with 100% illumination. The region between (y_b) and (y_m) presents illumination decreasing almost proportionally with the distance from (y_b) to (y_m). The region after (y_m) got 0% illumination.

Results of simulation of energy distribution using the proposed model is compared with results obtained using Evans' model [4] (Fig. 8). For this comparison it is used a parabola with a rim angle of (60 deg) and focal length (1m). The solar bright distribution was considered constant in the simulations. In Fig. 8 the abscissa axis has been expressed by a dimensionless variable y/f. The green curve represents the Evans´s model and the blue the proposed model.

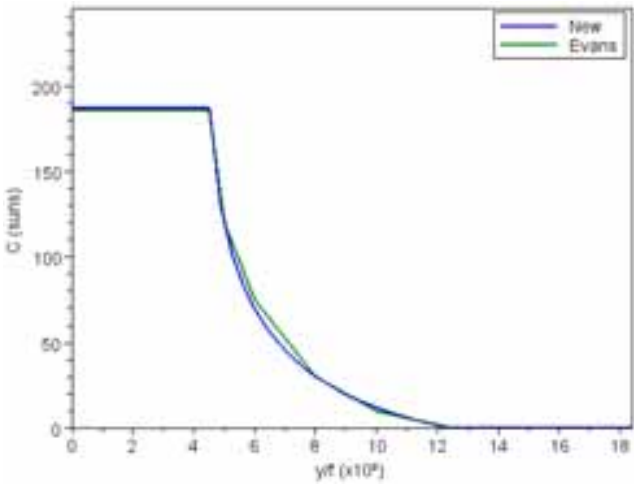

Fig. 8 – Comparison to the Evans´s model [5], it was used the constant bright distribution.

It can be observed that the two distributions are equivalent; the maximum value obtained was 185 suns in both models. The average value obtained from the graphs was 90.6 suns. The mean value calculated from the eq. 7 is very similar (91.3 suns).

4. Conclusions

It was presented in this paper an alternative and exact solution to obtain the energy distribution in a flat absorber of a linear parabolic collector.

A space ($\theta - \varphi$) was defined to allow visualizing the concentrator geometrical behavior for any bright distribution incident in the collector aperture. A function $\varphi = \varphi(\theta,y)$ or its inverse $\theta = \theta(\varphi,y)$ was developed, where (y) is represented by isolines in the space ($\theta - \varphi$).

The described procedure is general; it can be applied with any reflector surface geometry since it has only one reflection. It also permits to analyze and visualize the bright distribution effect over the energy distribution profile. The simplicity of the solution also allows considerations of optical deviation and misalignment´s effects over the image in the focal region. The implementation of these conditions, different from the ideal case, is being conducted and will be presented in a future work.

Acknowledgments: The authors would like to thank the Conselho Nacional de Desenvolvimento Científico e Tecnológico – CNPq for the support given to this research.

5. References

[1] Abetti, G., 1938. The Sun. D. Van Nostrand, Princeton, New Jersey.

[2] Daly, J. C., 1979. Solar concentrator flux distributions using backward ray tracing. Applied Optics, 18, 15.

[3] Duffie, J. A., Beckman, W. A., 1991. Solar engineering of thermal processes. 2ª ed., Wiley-Interscience, New York.

[4] Evans, D. L., 1977. On the performance of cylindrical parabolic solar concentrators with flat absorbers. Solar Energy, 19, 379 – 385.

[5] Fraidenraich, N, 2010. A new approach to calculate the energy distributions in solar concentrators. Lecture Notes, UFPE.

[6] Löf, G. O. G., Duffie, J. A., 1963. Optimization of focusing solar-collector design. J. Eng. Power Trans. ASME 85A, 221-227.

[7] Nicolás, R. O., Durán, J. C., 1980. Generalization of the two-dimensional optical analysis of cylindrical concentrators. Solar Energy, 25, 21-31.

[8] Pedrosa Filho, M. H. O., Vilela, O. C., Fraidenraich N., 2010. Avaliação da influência dos desvios ópticos e de rastreamento na concentração de coletor parabólico linear. Avances en Energías Renovables y Medio Ambiente, 14, 04-101.

[9] Rabl, A., 1985. Active solar collectors and their applications. New York: Oxford University Press.

[10] Rabl, A., Bendt, P., 1982. Effect of circunsolar radiation on performance of focusing collectors, J. Solar Energy Eng., 104, 237.